Neuropeptide AF induces piecemeal degranulation in murine mucosal mast cells : a new mediator in neuro-immune communication in the intestinal lamina propria?

Reference:
Abdellah Nada, Van Remoortel Samuel, Mohey-Elsaeed Omnia, Mustafa Mohamed-Nabil, Ahmed Yasser A., Timmermans Jean-Pierre, Buckinx Roeland.- Neuropeptide AF induces piecemeal degranulation in murine mucosal mast cells : a new mediator in neuro-immune communication in the intestinal lamina propria?
The anatomical record: advances in integrative anatomy and evolutionary biology - ISSN 1932-8486 - 301:6(2018), p. 1103-1114
Full text (Publisher's DOI): https://doi.org/10.1002/AR.23780

Neuropeptide AF induces piecemeal degranulation in murine mucosal mast cells: a new mediator in neuro-immune communication in the intestinal lamina propria?

Nada Abdellah[1, 2], Samuel Van Remoortel[2], Omnia Mohey-Elsaeed[2, 3], Mohamed-Nabil Mostafa[4], Yasser A. Ahmed[5] Jean-Pierre Timmermans[2], Roeland Buckinx[2]

[1]*Histology Department, Faculty of Veterinary Medicine, Sohag University, Sohag, Egypt.*

[2]*Laboratory of Cell Biology & Histology, University of Antwerp, Antwerp, Belgium.*

[3]*Department of Cytology and Histology, Faculty of Veterinary Medicine, Cairo University, Giza 12122, Egypt.*

[4]*Department of Anatomy and Histology, Faculty of Veterinary Medicine, Assiut University, Assiut, Egypt*

[5]*Department of Histology, Faculty of Veterinary Medicine, South Valley University, Qena, Egypt*

Correspondence to:

Prof. Dr. Jean-Pierre Timmermans

University of Antwerp

Laboratory of Cell Biology & Histology

Universiteitsplein 1

2610 Antwerp (Wilrijk), Belgium

jean-pierre.timmermans@uantwerpen.be

T: +32 3 265 33 27

F: +32 3 265 33 01

This article has been accepted for publication and undergone full peer review but has not been through the copyediting, typesetting, pagination and proofreading process which may lead to differences between this version and the Version of Record. Please cite this article as an 'Accepted Article', doi: 10.1002/ar.23780

Abstract

Neuropeptides AF (NPAF), FF (NPFF) and SF (NPSF) are RFamide neuropeptides known to be widely expressed in the mammalian central nervous system, where they fulfill a wide range of functions with pain modulation being the most prominent one. Recent evidence indicates that RFamides act as mediators in mast cell–sensory nerve communications related to allergic disease. Previous work by our group has shown that the expression levels of some members of the Mas-related gene receptor (Mrgpr) family in both enteric neurons and mucosal mast cells change during intestinal inflammation. The Mrgpr subtypes C11 and A4 can be activated by NPAF, while A1 and C11 are triggered by NPFF. The aim of the present study was to investigate whether RFamides of the NPFF group are expressed in the gastrointestinal tract and to identify possible targets and receptors that might be involved in RFamide-associated mast cell modulation. To this end, the expression and distribution patterns of NPFF/AF receptors and the NPFF precursor protein were determined in bone marrow-derived mucosal mast cells (BMMCs) by immunocytochemistry and (RT-)PCR. BMMCs were found to express MrgprA4 and A1, and functional analysis of the effects of NPAF by means of a β-hexosaminidase assay, mMCP-1 ELISA, electron microscopy and live cell calcium imaging revealed a piecemeal degranulation induced by NPAF. However, knock-out of MrgprA4 and A1 did not reduce the effect of NPAF, indicating that the BMMC response to NPAF was receptor independent. ProNPFF was expressed in neurons and BMMCs, suggesting that both cell types are potential sources of NPAF *in situ*. Our results show that the RFamide NPAF can be considered as a novel modulator of BMMC activity in the neuro-immune communication in the gastrointestinal tract, although the exact signaling pathway remains to be elucidated.

Keywords: Neuropeptide AF, RFamides, Mas-related gene receptor A4, Bone marrow-derived mucosal mast cells, Enteric neurons, Neuro-immune interaction

Introduction

Neuropeptides FF (NPFF), AF (NPAF), and SF (NPSF) (henceforth together referred to as "RFamides") are homologous amidated peptides that belong to a class of peptides known as FMRFamide-related peptides. They are derived from the same precursor protein, proNPFF, which is encoded by the Npff gene (Yang and Martin, 1995, Vilim et al., 1999), are widely distributed throughout the mammalian central nervous system and fulfill a wide range of functions (Panula, Aarnisalo et al. 1996, Merighi, Salio et al. 2011). Although anti-opiate effects (Tang et al., 1984, Malin et al., 1990) and related pain modulation (Yang et al., 1985; Gouardères et al., 1993) are the most prominent effects of FMRFamide-related peptides, RFamides are also implicated in cardiovascular regulation (Panula et al., 1996), food intake and intestinal motility. Furthermore, they play a role as mediators in mast cell–sensory nerve communication related to allergic disease, mainly through Mas-related gene receptor (Mrgpr) signaling, whereby connective tissue mast cells release RFamides that stimulate sensory neurons or these mast cells are activated by neuronal mediators (Tatemoto et al., 2006; Lee et al., 2008, 2011). Although most Mrgprs are orphans, NPAF has been found to act as a ligand of MrgprA4 (EC_{50} ~ 60 nM) and MrgprC11 (EC_{50} ~ 300 nM), while NPFF serves as a ligand for MrgprA1 (EC_{50} ~ 200-2000 nM) and MrgprC11 (EC_{50} ~ 60 nM). (Dong et al., 2001; Han et al., 2002). NPAF and NPFF also activate to the G protein-coupled receptors NPFF1 (NPFF: EC_{50} ~ 15-250 nM; NPAF: 25-325 nM) and NPFF2 (HLWAR77; NPFF: EC_{50} ~ 2 nM; NPAF: EC_{50} ~ 1-5 nM) (Bonini et al., 2000; Elshourbagy et al., 2000; Liu et al., 2001; Mollereau et al., 2002; Findeisen et al., 2011). Some Mrgprs have been suggested to play roles in the regulation of inflammatory

responses to non-immunological activation of mast cells and in mast cell–neuron communication in the gastrointestinal (GI) tract (Avula et al., 2013; Solinski et al., 2014). Yet, it remains unknown whether RFamides, just like in connective tissue mast cells, are capable of eliciting a response in mucosal mast cells (MMCs). The aim of this study was hence to investigate whether MMCs express receptors for RFamides and respond to these neuropeptides, be it as part of an autocrine loop or in response to RFamide release from other cellular sources within the intestinal lamina propria.

Materials and methods

Animals

Experiments were performed on adult male C57BL/6 wild-type mice and the Mrgpr-clusterΔ, Del(7Mrgpra1-Mrgprb4) cluster knockout (cluster-KO) mice (kindly provided by Dr. Dong, Johns Hopkins University) (Liu et al., 2009). Animal housing and handling procedures were conducted in accordance with the European Directive 86/609/EEC.

Bone marrow-derived mucosal mast cell cultures and morphological characterization

Bone marrow-derived mucosal mast cell (BMMC) cultures were generated following previously described methods (Miller et al., 1999; Wright et al., 2002, De Jonge et al., 2004). Cell cultures were set up in a humid 5% CO_2 incubator at 37°C, fed at 2- to 3-day intervals and maintained for up to 14 days. The cells showed morphological and functional characteristics resembling those of MMCs after 9 days in culture (Miller et al., 1999; Wright et al., 2002; De Jonge et al., 2004). To follow the selective enrichment of the culture in pure BMMCs, samples

from the culture were collected at 2-day intervals starting at 8 days. The presence of dense-cored granules and the expression of mMCP-1 in the cultured cells were examined using Leishman's staining and immunofluorescence (supplementary figure 1). Cells were fixed in modified Bouin's solution for 10 min and permeabilized in absolute methanol for 10 min at room temperature, before being stored at -80°C until further processing for immunocytochemistry. Fixed cells were immersed in 0.01M PBS containing 10% normal horse serum, 0.01% bovine serum albumin, 0.05% thimerosal and 0.01% sodium azide (PBS*) to which 1% Triton X-100 was added. Next, they were incubated overnight with a primary antibody in PBS*. Subsequently, after being rinsed in PBS, the tissue was incubated with an appropriate secondary antibody for 2 hrs in PBS*. The primary and secondary antibodies are listed in Table 1. All incubations were performed at room temperature. Slides were enclosed and studied under a fluorescence microscope.

RNA isolation, reverse transcriptase (RT)-PCR

RT-PCR was used to identify the expression of the proNPFF gene, Npff, in dorsal root ganglia, myenteric neurons, and BMMCs and of murine Mrgpra1, Mrgpra4, Mrgprc11 (= Mrgprx1), and Npffr1 and Npffr2 in BMMCs. Total RNA was isolated using the NucleoSpin RNA kit (Macherey-Nagel) following the manufacturer's protocol. Following isolation, the integrity of the isolated RNA samples was evaluated and their concentration was determined by the Agilent Bioanalyzer using the Agilent RNA 6000 Nano Kit (Agilent Technologies). Next, a total amount of 500 ng DNase-treated RNA was reverse-transcribed using the SuperScript cDNA Synthesis kit (BioRad). The primers used for RT-PCR were either self-designed using the PrimerBLAST program (www.ncbi.nlm.nih.gov/tools/primer-blast) or commercially obtained PrimePCR assays (BioRad) (Table 2). All primers are exon spanning, except for Mrgpra4, and

gradient PCR was performed first to estimate the proper annealing temperature (T^A) for each self-designed primer. RT-PCR was performed on 1 µl cDNA of each sample. Non-reverse-transcribed controls and blank control samples (containing no template) were incorporated in the assay to exclude possible contamination in case of positive signal. Positive control samples were incorporated to confirm PCR reaction efficiency.

Tissue processing for immunohistochemistry

Tissues of interest were fixed in 4% paraformaldehyde for 2 hrs. For cryosections, the tissues were incubated overnight in 20% sucrose prior to being embedded and frozen in cryo-embedding compound (Pelko Int., Torrance, CA, USA), and immediately processed for cryosectioning or stored at -80 °C until further use. Ten-micrometer-thick frozen sections were made using a cryostat (Leica CM1950, Leica). The sections were collected on poly-L-lysine-coated slides. In a final step, the slides were dried for at least 2 hrs at 37°C prior to further use for immunohistochemical staining. For whole-mount preparations, intestinal segments were processed as described earlier (Avula et al., 2013). The procedure for immunofluorescent staining of cryosections and whole-mounts was analogous to the above-described protocol for BMMC immunocytochemistry. Primary and secondary antibodies are listed in Table 1. Cryosections and whole-mounts were evaluated with a microlens-enhanced dual spinning confocal microscope (UltraView Vox, PerkinElmer Inc., Waltham, MA, USA).

Electron microscopy

At 14 days *in vitro*, BMMCs were divided into three treatment groups: the first group was stimulated with C48/80 (20ug/ml), the second stimulated with NPAF (300 nM) (30 min at 37°C) and the third group was left unstimulated. Culture samples (3 ml) were centrifuged at 250g for 7

min. The supernatant was removed and the pellet was fixed with 0.1 M cacodylate-buffered 2% glutaraldehyde (pH 7.4). Subsequently, the pellet was broken into small pieces and postfixed in 0.1 M cacodylate-buffered 1% osmium tetroxide, followed by dehydration in acetone prior to embedding in Durcupan. After 2 days, 50-nm-thin sections were cut and contrasted with 2% uranyl acetate and Reynold's solution for 10 min. The sections were then analyzed in a Tecnai G2 Spirit BioTWIN transmission electron microscope (Fei Company, Eindhoven, The Netherlands).

β-hexosaminidase release assay

At 14 days *in vitro*, $1x10^5$ BMMCs were resuspended in HEPES buffer and seeded into a 96-well plate for incubation with 300 nM, 600 nM, or 1 μM NPAF. We used 4 technical replicates for each sample and 4 biological replicates (4 cultures) in total. After 30 min of incubation, the cells were centrifuged at 450 g, 4°C for 5 min, the supernatant was collected and the cells were lysed in 0.1% Triton X-100 solution. Ten microliters of 4-nitrophenyl n-acetyl-β-d-glucosaminide (Sigma-Aldrich) solution in citrate buffer was added to an equal volume of supernatant or cell lysate and incubated for 90 min at 37°C. The enzymatic reaction was stopped by addition of 50 μl of 400 mM glycine in each well. Absorbance was measured at 405 nM with the reference filter at 620 nm. Spontaneous release of β-hexosaminidase was measured by incubating the cells in HEPES buffer alone and C48/80 was included as positive control. The percentage of β-hexosaminidase released in response to NPAF stimulation was normalized to the total amount of β-hexosaminidase present in the cell lysate and supernatant.

ELISA-based mMCP-1 release assay

The release of mMCP-1 from BMMCs after stimulation with NPAF was measured using an ELISA Kit (Mouse MCPT-1 ELISA Ready-SET-Go, eBioscience). NPAF concentrations ranging from 50 nM to 600 nM were tested. Each sample was run in duplicate, with samples of 4 biological replicates (4 cultures). All experiments were performed as per the manufacturer's guidelines. The released amount of mMCP-1 was calculated using a standard curve, and unstimulated BMMCs were considered baseline. C48/80 was included as positive control.

Calcium live cell imaging

Intracellular calcium mobilization was recorded on a microlens-enhanced dual spinning disk confocal system (UltraView ERS, PerkinElmer). 1.10^6 BMMCs were washed, resuspended in 400 µl DMEM-F12 buffer and seeded in 100 µl onto the poly-L-lysine-coated bottom of a well (diameter 10 mm) in a 35-mm-diameter culture dish (MatTek, Ashland, MA, USA). Cells were then left to settle to the bottom for 30 min and subsequently incubated with the Ca2+ indicator dye Fluo-4 AM (1 µM; Molecular Probes, Invitrogen, Carlsbad, CA, USA) in DMEM F-12 buffer at 37°C for 30 min. After stopping the dye loading by refreshing the buffer, the dishes were transferred to the microscope stage. At 5 min from the start of the recording, NPAF was added from a micropipette to a final concentration of 300 nM. C48/80 (20ug/ml) was added after the second 5 min as a positive control to give an indication of the viability and reactivity of the BMMCs. Cells that were unresponsive to C48/80 were excluded from further analysis. To exclude that the cells have a mechanical response to pipetting, DMEM F-12 buffer without compounds was pipetted at 2 min from the start of the recording. Live cell experiments were performed at RT. Time-lapse images of Fluo-4 fluorescence were recorded at 2 Hz by 488-nm laser excitation and FITC emission filter detection. Image analysis was done offline with Velocity 2 software (Improvision, Coventry, UK) by drawing a region of interest (ROI) around

each individual cell. For each ROI, the fluorescence intensity is expressed as an arbitrary unit of time. To determine the response of BMMCs to NPAF, the frequency of Ca^{2+} oscillations and the area under the curve were measured before and after NPAF application.

Statistical analysis

Data are presented as the mean ± SEM. Statistical tests are specified in the appropriate results section. Differences were considered significant at (***$P \leq 0.001$, **$P \leq 0.01$ and *$P \leq 0.05$).

Results

Identification of possible sources of RF-amides

Possible RF-amide sources were identified in intrinsic and extrinsic components of the enteric nervous system. RT-PCR analysis detected the presence of mRNA of the precursor proNPFF in dorsal root ganglia, myenteric neurons and BMMCs (Fig. 1), implicating these cell types as potential sources of RFamides.

Subsequently, the presence of FMRFamide in the ileal and colonic wall was verified by immunohistochemistry. In the absence of a specific antibody for NPAF, NPFF or proNPFF, the tissue was immunostained for FMRFamide. Negative controls, in which the primary antibody was omitted or staining was done with IgG control, did not yield any immunoreactivity. Immunofluorescent staining against FMRFamide on cryosections of ileum and colon clearly revealed an enteroendocrine cell morphology with a prominent cytoplasmic process known as a neuropod (Figs. 2A-D). Immunostained whole-mount preparations from ileal and colonic

segments demonstrated the expression of FMRFamide in nerve fibers within both the submucosal and the myenteric plexus (Figs. 2E,F), but not in intrinsic neuronal somata, not even after colchicine treatment, a classical method to enhance perikaryal staining of neuropeptides by inhibiting axonal transport (Fig. 2G). Double staining of FMRFamide-positive nerve fibers with anti-CGRP or anti-tyrosine hydroxylase revealed colocalization with the latter (indicative of an extrinsic postganglionic sympathetic origin), but not with CGRP (a marker for viscerosensory neurons) (Figs. 3A-L).

Expression of receptors for proNPFF products in BMMCs

RT-PCR analysis revealed the presence of Mrgpra4 and Mrgpra1, but not of Mrgprc11 (Fig. 4) and detected no mRNA of Npffr1 and Npffr2 in BMMCs (Fig. 4). Identical results were obtained in four different BMMC cultures (derived from distinct animals). The presence of MrgprA4 was confirmed at the protein level by immunocytochemical staining of BMMCs for the MrgprA4 receptor (Fig. 5A). Method specificity was checked by omission of the primary antibody resulting in no staining (Fig. 5B). An antiserum for MrgprA1 is not available.

Transmission electron microscopy (TEM)

Although most Mrgprs are orphans, MrgprA4 is known to be activated by NPAF. To assess the response of individual BMMCs to NPAF, possible ultrastructural changes in BMMCs in response to stimulation with NPAF were examined by TEM. Unstimulated cells were packed with electron-dense granules (Fig. 6A); cells stimulated with NPAF (300 nM) for 30 min displayed partial loss of their granule content reminiscent of piecemeal degranulation (Fig. 6B), while cells stimulated with C48/80 (20 ug/ml) showed a further substantial loss of their granule content (Fig. 6C).

Mediator release in response to NPAF

Considering that piecemeal degranulation involves selective mediator release, we next assessed possible changes in the release of two classic mast cell mediators, ß-hexosaminidase, and mMCP-1, following stimulation with NPAF. NPAF stimulation led to the release of 6.62±2.9% (300 nM), 7.48±1.34% (600nM) and 7.27±1.98% (1uM) of total cellular ß-hexosaminidase (n=5) (Fig.7A), i.e. a small but significant increase compared to baseline levels of ß-hexosaminidase release (4.21±0.78%, p=0.043, n=5 cultures, one-way ANOVA). In contrast, degranulation by C48/80 triggered the release of 48.99±9.38% of total cellular ß-hexosaminidase (Fig. 7B).

ELISA analysis of mMCP-1 release after NPAF stimulation (50, 100, 150, 300, and 600 nM) showed a NPAF concentration-dependent increase in mMCP-1 concentration in the culture supernatant. All values were within the dynamic range of the standard curve and the release of mMCP-1 was normalized to that of unstimulated BMMCs (Fig. 8). The highest concentration of NPAF (600 nM) led to a mMCP-1 release of 5936.5±323.2 pg/ml (n=4 cultures) compared to a release of 32,553.1±2,342.0 pg/ml (n=4 cultures) following C48/80 application.

Live cell calcium imaging

Calcium imaging using Fluo-4 was performed to assess the response of individual BMMCs to NPAF (300 nM). C48/80 was subsequently added as a control of mast cell activation/degranulation. No changes were detected after application of medium only. However, BMMCs responded with an increase in $Ca2^{+}$ oscillations following NPAF application and with a sudden increase in intracellular Ca^{2+} followed by degranulation after application of C48/80 (Figs. 9,10). Ca^{2+} peak frequency was 1.50 ± 0.08-fold increased compared to the control situation

(0.91± 0.22/min before NPAF stimulation vs. 1.32±0.27 after NPAF stimulation, n=5 cultures) (Figs. 11A-C). To verify whether the observed NPAF effect was mediated through the MrgprA4 receptor, BMMCs were obtained from the cluster-KO mice. Live cell imaging analysis showed that the Ca^{2+} peak frequency was still significantly enhanced and that the NPAF effect, with a 1.53±0.17-fold increase compared to controls, was comparable to the increase seen in WT cultures (Figs. 11C-D) following treatment with 300 nM NPAF (0.56±0.13 vs. 0.82±0.11 peaks/min, n=3 KO cultures). Repeated measures ANOVA confirmed that "NPAF treatment (p=0.001)" but not "genotype (cluster-KO; p=0.25)" had a significant influence on peak frequency. Likewise, the ratio of the area under the curve before NPAF stimulation to that after NPAF stimulaton was not significantly different either between WT (1.46 ± 0.08) versus cluster-KO cultures (1.67± 0.10) (unpaired t-test after log-normal data transformation, p = 0.155).

Discussion

The present study was undertaken to determine the sources of RFamides in the GI tract and investigate the response of MMCs to these neuropeptides (Tatemoto et al., 2006). To this end, BMMCs were generated in vitro, yielding cells with morphological and functional characteristics resembling those of MMCs (Miller et al., 1999; Wright et al., 2002; De Jonge et al., 2004)

The NPAF precursor proNPFF is transcriptionally expressed in dorsal root ganglia, primary myenteric neurons and BMMCs. In agreement with our results, proNPFF has been detected before in mouse connective tissue mast cells (Lee et al., 2008). This expression in

BMMCs suggests a possible autocrine feedback loop. Such neuropeptide expression in mast cells and positive feedback potential has been described before, e.g. for vasoactive intestinal peptide or substance P (Tore & Tuncel 2009). Previous studies have shown that NPFF and NPAF, and likely other RFamide peptides, can be detected by an anti-FMRFamide antibody (Lee et al., 2008). We therefore used this antibody to identify the potential sources of RFamides *in situ*, revealing the presence of RFamide peptides in enteroendocrine cells and nerve fibers located in the ganglionic plexuses of both ileum and colon. We regularly observed so-called 'neuropods' on the FMRFamide-immunoreactive enteroendocrine cells (Bohórquez et al., 2011, 2014, 2015), although contacts of these neuropods with immune cells have not yet been explored. Although we do know that FMRFamide is the most abundant neuropeptide in the alimentary tract of insects (Oetken et al., 2004; Haselton et al., 2008), nothing is currently known about the expression and function of RFamides in the mammalian GI tract. In our study double immunostainings of ileal and colonic whole-mounts revealed that RFamide peptides were expressed in tyrosine hydroxylase-positive nerve fibers, indicative of extrinsic postganglionic sympathetic axons. Despite expression of FMRFamide in dorsal root ganglia, CGRP-immunoreactive nerve fibers, indicative of either intrinsic or extrinsic afferent fibers, did not colocalize with FMRFamide-immunoreactive nerve fibers in the intestinal wall. Although these results identify possible sources of FMRFamide-related peptides, follow-up experiments must further explore the existence of this direct cell-to-cell signaling before making definite claims. Furthermore, given that BMMCs express proNPFF, inflammatory phenomena such as mastocytosis might provide additional sources for FMRFamide-related peptides.

We next searched for possible receptors for proNPFF products in BMMCs using RT-PCR. Our results showed that BMMCs expressed MrgprA4 and MrgprA1, but not MrgprC11 or

mRNA of NPFF1 and NPFF2. Based on these data we next analyzed the effect of NPAF on BMMCs and found that BMMCs responded to NPAF concentrations that are within the normal pharmacological range of known NPAF receptors (Bonini et al., 2000; Elshourbagy et al., 2000; Dong et al., 2001; Han et al., 2002; Mollereau et al., 2002; Findeisen et al., 2011).

First, our TEM results showed that NPAF stimulation led to a partial loss of the cytoplasmic granule density in BMMCs, pointing to piecemeal degranulation, a secretory pathway during which mast cells differentially release mediators (Theoharides et al., 2007). Similar ultrastructural changes reminiscent of piecemeal degranulation were observed in CGRP-mediated BMMC activation (De Jonge et al., 2004, Rychter et al., 2011). In contrast, C48/80-mediated BMMC activation resulted in a complete degranulation corresponding to a total release of mast cell mediators (De Jonge et al., 2004, Theoharides et al., 2007).

Second, in line with our TEM findings, incubation of BMMCs with NPAF for 30 min induced a marginal release of the granule-associated mediator β-hexosaminidase and a clear dose-dependent release of mMCP-1. This differential mediator release and the observation that the maximal mMCP-1 release following NPAF stimulation merely accounted for 20% of the mMCP-1 release seen after C48/80 stimulation, lend further support to the piecemeal degranulation pathway. The differential release of mediators is well described in the case of piecemeal degranulation. Our own previous work showed a similar effect of CGRP on BMMCs (Rychter et al. 2011). However, the exact cell biological mechanisms involved in this differential mediator release are not well understood (Theoharides et al. 2007; Moon et al. 2014).

Third, in agreement with the TEM and mediator release results, NPAF induced an increase in the Ca^{2+} oscillation frequency of BMMCs. The presence of Ca^{2+} oscillations is a well-documented phenomenon in multiple mast cell types (Parekh 2011; Cohen et al., 2012;

Wilkes et al., 2014). A similar observation of a wavy Ca^{2+} oscillation pattern has been reported in FcRI-activated rat bone marrow-derived mast cells (Cohen et al., 2009). The subtle changes in Ca^{2+} oscillations observed here differ from the classic C48/80-induced degranulation involving a sudden rise in intracellular Ca^{2+} levels, as previously also seen in Fluo-4-loaded BMMCs (De Jonge et al., 2004; Rychter et al., 2011) and connective tissue mast cells (McNeil et al., 2015).

In order to identify whether the NPAF-associated piecemeal degranulation is induced through MrgprA4, we proceeded to perform Ca^{2+} imaging experiments on BMMCs isolated from the Mrgpr-clusterΔ KO mice, which lack expression of MrgprA4, amongst other Mrgprs (Liu et al., 2009). However, the NPAF-induced changes in Ca^{2+} oscillation frequency remained comparable to those in WT mice, suggesting that the BMMC response to NPAF is mediated neither by Mrgprs nor by NPFF receptors (which were not expressed). The question hence arises whether a new, so far unidentified receptor might be involved, which would not be surprising given the large number of orphan G protein-coupled receptors, even within the Mrgpr family (Tang et al., 2012; Solinski et al., 2014). Similarly, MMC degranulation by the neuropeptide substance P was initially thought to be a non-receptor-dependent response (Maggi, 1997) until later studies revealed that substance P can stimulate murine mast cells via the neurokinin 1 receptor (van der Kleij et al., 2003) and human mast cells via MrgprX2 (Tatemoto et al., 2006). Likewise, CGRP and C48/80 initially were suggested to activate mast cells via membrane-associated receptor-independent stimulation of Gi-like proteins (Mousli et al., 1994; Ferry et al., 2002; De Jonge et al., 2004). Recently, it has been reported that murine BMMCs can be activated by CGRP via CGRP1 receptors (Rychter et al., 2011) and C48/80 activates mast cells through MrgprB2 (McNeil et al., 2015). CGRP and substance P are both basic secretagogues. It is clear that these types of compounds activate G proteins in mast cells, but whether this is a

GPCR-mediated process, a direct interaction with G proteins or a combination of both remains a matter of debate (Heifetz et al., 2015). Comparison of the isoelectric point (IP) of NPAF (6.759) with those of CGRP (8.83) and substance P (10.61) shows that CGRP and substance P are positively charged within the cytoplasm, while NPAF is neutral, rendering it unlikely that NPAF activates BMMCs through the same signaling pathway as both basic secretagogues.

In conclusion, we propose that NPAF originating from enteroendrocrine cells or sympathetic innervation may influence MMCs in the intestine by inducing a piecemeal degranulation involving the release of mast cell proteases. This, in turn, could contribute to neuronal sensitization and to hypersensitivity in GI pathology, such as irritable bowel syndrome, as has been described earlier for other neuropeptides including CGRP and VIP (Van Nassauw et al., 2007; van Diest et al., 2012). The role of NPAF-mediated mast cell modulation *in vivo* should thus be the subject of follow-up studies.

Acknowledgements.

This study has been supported by research grant G019314N of the Research Fund – Flanders (FWO) and by BOF-GOA project 28313 of the University of Antwerp.

References

Avula LR, Buckinx R., Favoreel H, Cox E, Adriaensen D, Van Nassauw L, Timmermans J-P. 2013. Expression and distribution patterns of Mas-related gene receptor subtypes A–H in the mouse intestine: inflammation-induced changes. Histochemistry and cell biology 139(5): 639-658.

Bohórquez DV, Chandra R, Samsa LA, Vigna SR, Liddle RA. 2011. Characterization of basal pseudopod-like processes in ileal and colonic PYY cells. Journal of molecular histology 42(1): 3-13.

Bohórquez DV, Samsa LA, Roholt A, Medicetty S, Chandra R, Liddle RA. 2014. An enteroendocrine cell–enteric glia connection revealed by 3D electron microscopy. PloS one 9(2): e89881.

Bohórquez DV, Shahid RA, Erdmann A, Kreger AM, Wang Y, Calakos N, Wang F, Liddle RA. 2015. Neuroepithelial circuit formed by innervation of sensory enteroendocrine cells. The Journal of clinical investigation 125(2): 782-786.

Bonini JA, Jones KA, Adham N, Forray C, Artymyshyn R, Durkin MM, Smith KE, Tamm JA, Boteju LW, Lakhlani PP. 2000. Identification and characterization of two G protein-coupled receptors for neuropeptide FF. Journal of Biological Chemistry 275(50): 39324-39331.

Cohen R, Corwith K, Holowka D, Baird B. 2012. Spatiotemporal resolution of mast cell granule exocytosis reveals correlation with Ca2+ wave initiation. J Cell Sci 125(Pt 12): 2986-2994.

Cohen R, Torres A, Ma H-T, Holowka D, Baird B. 2009. Ca2+ Waves Initiate Antigen-Stimulated Ca2+ Responses in Mast Cells. The Journal of Immunology 183(10): 6478-6488.

De Jonge F, De Laet A, Van Nassauw L, Brown J, Miller H, Van Bogaert P-P, Timmermans J-P, Kroese A, 2004. In vitro activation of murine DRG neurons by CGRP-mediated mucosal mast cell degranulation. American Journal of Physiology-Gastrointestinal and Liver Physiology 287(1): G178-G191.

Dong X, Han S-K, Zylka MJ, Simon MI, Anderson DJ. 2001. A Diverse Family of GPCRs Expressed in Specific Subsets of Nociceptive Sensory Neurons. Cell 106(5): 619-632.

Elshourbagy NA, Ames RS, Fitzgerald LR, Foley JJ, Chambers JK, Szekeres PG, Evans NA, Schmidt DB, Buckley PT, Dytko GM. 2000. Receptor for the pain modulatory neuropeptides FF and AF is an orphan G protein-coupled receptor. Journal of Biological Chemistry 275(34): 25965-25971.

Ferry X, Brehin S, Kamel R, Landry Y. 2002. G protein-dependent activation of mast cell by peptides and basic secretagogues. Peptides 23(8): 1507-1515.

Findeisen M, Rathmann D, Beck-Sickinger AG. 2011. RFamide Peptides: Structure, Function, Mechanisms and Pharmaceutical Potential. Pharmaceuticals 4(9): 1248-1280.

Gouardères C, Sutak M, Zajac J-M, Jhamandas K. 1993. Antinociceptive effects of intrathecally administered F8Famide and FMRFamide in the rat. European journal of pharmacology 237(1): 73-81.

Han S-K, Dong X, Hwang J-I, Zylka MJ, Anderson DJ, Simon MI. 2002. Orphan G protein-coupled receptors MrgA1 and MrgC11 are distinctively activated by RF-amide-related peptides through the Gαq/11 pathway. Proceedings of the National Academy of Sciences 99(23): 14740-14745.

Haselton AT, Yin CM, Stoffolano JG. 2008. FMRFamide-like immunoreactivity in the central nervous system and alimentary tract of the non-hematophagous blow fly, Phormia regina, and the hematophagous horse fly, Tabanus nigrovittatus. J Insect Sci 8: 1-17.

Heifetz A, Schertler GFX, Seifert R, Tate CG, Sexton PM, Gurevich VV, Fourmy D, Cherezov V, Marshall FH, Storer RI, Moraes I, Tikhonova IG, Tautermann CS, Hunt P, Ceska T, Hodgson S, Bodkin MJ, Singh S, Law RJ, Biggin PC. 2015. GPCR structure, function, drug discovery and crystallography: report from Academia-Industry International Conference (UK Royal Society) Chicheley Hall, 1–2 September 2014. Naunyn-Schmiedeberg's Archives of Pharmacology 388(8): 883-903.

van der Kleij HP, Ma D, Redegeld FA. 2003. Functional expression of neurokinin 1 receptors on mast cells induced by IL-4 and stem cell factor. J Immunol 171: 2074-2079.

Lee M-G, Dong X, Liu Q, Patel KN, Choi OH, Vonakis B, Undem BJ. 2008. Agonists of the Mas-Related Gene (Mrgs) Orphan Receptors as Novel Mediators of Mast Cell-Sensory Nerve Interactions. The Journal of Immunology 180(4): 2251-2255.

Lee, M-G, Park J-Y, Park YK, Undem BJ. 2011. Direct Activation of Guinea Pig Vagal Afferent Neurons by FMRFamide. Neuroreport 22(12): 609-612.

Liu Q, Guan XM, Martin WJ, McDonald TP, Clements MK, Jiang Q, Zeng Z, Jacobson M, Williams Jr. DL, Yu H, Bomford D, Figueroa D, Mallee J, Wang R, Evans J, Gould R, Austin CP. 2001. Identification and characterization of novel mammalian neuropeptide FF-like peptides that attenuate morphine-induced antinociception. J Biol Chem 276(40): 36961-36969.

Liu Q, Tang Z, Surdenikova L, Kim S, Patel KN, Kim A, Ru F, Guan Y, Weng H-J, Geng Y, Undem BJ, Kollarik M, Chen Z-F, Anderson DJ, Dong X. 2009. Sensory Neuron-Specific GPCR Mrgprs Are Itch Receptors Mediating Chloroquine-Induced Pruritus. Cell 139(7): 1353-1365.

Maggi CA. 1997. The effects of tachykinins on inflammatory and immune cells. Regul Pept 70: 75-90.

Malin DH, Lake JR, Hammond MV, Fowler DE, Leyva JE, Rogillio RB, Sloan JB, Dougherty TM, Ludgate K. 1990. FMRF-NH2 like mammalian octapeptide in opiate dependence and withdrawal. Problems of Drug Dependence 1990 Proceeding of the 52nd Annual Scientific Meeting.

McNeil BD, Pundir P, Meeker S, Han L, Undem BJ, Kulka M, Dong X. 2015. Identification of a mast-cell-specific receptor crucial for pseudo-allergic drug reactions. Nature 519(7542): 237-241.

Merighi A, Salio C, Ferrini F, Lossi L. 2011. Neuromodulatory function of neuropeptides in the normal CNS. J Chem Neuroanat 42(4): 276-287.

Miller HR, Wright SH, Knight PA, Thornton EM. 1999. A novel function for transforming growth factor-β1: upregulation of the expression and the IgE-independent extracellular release of a mucosal mast cell granule-specific β-chymase, mouse mast cell protease-1. Blood 93(10): 3473-3486.

Mollereau C, Mazarguil H, Marcus D, Quelven I, Kotani M, Lannoy V, Dumont Y, Quirion R, Detheux M, Parmentier M, Zajac J-M. 2002. Pharmacological characterization of human NPFF1 and NPFF2 receptors expressed in CHO cells by using NPY Y1 receptor antagonists. European Journal of Pharmacology 451(3): 245-256.

Moon TC, Befus AD, Kulka M. 2014. Mast cell mediators: their differential release and the secretory pathways involved. Front Immunol 5(article 569): 1-18.

Mousli M, Hugli T, Landry Y, Bronner C. 1994. Peptidergic pathway in human skin and rat peritoneal mast cell activation. Immunopharmacology 27(1): 1-11.

Oetken M, Bachmann J, Schulte-Oehlmann U, Oehlmann J. 2004. Evidence for endocrine disruption in invertebrates. Int Rev Cytol 236: 1-44.

Panula P, Aarnisalo AA, Wasowicz K. 1996. Neuropeptide FF, a mammalian neuropeptide with multiple functions. Progress in Neurobiology 48(4–5): 461-487.

Parekh AB. 2011. Decoding cytosolic Ca2+ oscillations. Trends Biochem Sci 36(2): 78-87.

Rychter JW, Van Nassauw L, Timmermans J-P, Akkermans L, Westerink R, Kroese A. 2011. CGRP1 receptor activation induces piecemeal release of protease-1 from mouse bone marrow-derived mucosal mast cells. Neurogastroenterology & Motility 23(2): e57-e68.

Solinski HJ, Gudermann T, Breit A. 2014. Pharmacology and Signaling of MAS-Related G Protein–Coupled Receptors. Pharmacological reviews 66(3): 570-597.

Tang J, Yang H, Costa E. 1984. Inhibition of spontaneous and opiate-modified nociception by an endogenous neuropeptide with Phe-Met-Arg-Phe-NH2-like immunoreactivity. Proceedings of the National Academy of Sciences 81(15): 5002-5005.

Tang XL, Wang Y, Li DL, Luo J, Liu MY. 2012. Orphan G protein-coupled receptors (GPCRs): biological functions and potential drug targets. Acta Pharmacol Sin 33(3): 363-371.

Tatemoto K, Nozaki Y, Tsuda R, Konno S, Tomura K, Furuno M, Ogasawara H, Edamura K, Takagi H, Iwamura H, Noguchi M, Naito T. 2006. Immunoglobulin E-independent activation of mast cell is mediated by Mrg receptors. Biochemical and Biophysical Research Communications 349(4): 1322-1328.

Theoharides TC, Kempuraj D, Tagen M, Conti P, Kalogeromitros D. 2007. Differential release of mast cell mediators and the pathogenesis of inflammation. Immunological Reviews 217(1): 65-78.

Tore F, Tuncell N. 2009. Mast cells: target and source of neuropeptides. Curr Pharm Des 15(29): 3433-3445

van Diest SA, Stanisor OI, Boeckxstaens GE, de Jonge WJ, van den Wijngaard RM. 2012. Relevance of mast cell-nerve interactions in intestinal nociception. Biochim Biophys Acta 1822(1): 74-84.

Van Nassauw L, Adriaensen D, Timmermans J-P. 2007. The bidirectional communication between neurons and mast cells within the gastrointestinal tract. Autonomic Neuroscience 133(1): 91-103.

Vilim FS, Aarnisalo AA, Nieminen M-L, Lintunen M, Karlstedt K, Kontinen VK, Kalso E, States B, Panula P, Ziff E. 1999. Gene for Pain Modulatory Neuropeptide NPFF: Induction in Spinal Cord by Noxious Stimuli. Molecular Pharmacology 55(5): 804-811.

Wilkes MM, Wilson JD, Baird B, Holowka D. 2014. Activation of Cdc42 is necessary for sustained oscillations of Ca2+ and PIP2 stimulated by antigen in RBL mast cells. Biol Open 3(8): 700-710.

Wright S, Brown J, Knight P, Thornton E, Kilshaw P, Miller H. 2002. Transforming growth factor-bβ1 mediates coexpression of the integrin subunit aαE and the chymase mouse mast cell protease-1 during the early differentiation of bone marrow-derived mucosal mast cell homologues. Clinical & Experimental Allergy 32(2): 315-324.

Yang H, Martin R. 1995. Isolation and characterization of a neuropeptide FF-like peptide from brain and spinal cord of rat. Soc Neurosci Abstr 21(1-3):760

Yang HY, Fratta W, Majane EA, Costa E. 1985. Isolation, sequencing, synthesis, and pharmacological characterization of two brain neuropeptides that modulate the action of morphine. Proceedings of the National Academy of Sciences of the United States of America 82(22): 7757-7761.

Figure Legends.

Fig. 1. mRNA for the NPAF precursor proNPFF is expressed in dorsal root ganglia, myenteric neurons and BMMCs (NRT: No Reverse Transcriptase reaction)

Fig. 2. Anti-FMRFamide-stained cryosections and whole-mounts. (A-B) Cryosections of colon (A) and ileum (B) showing expression of FMRFamides in enteroendocrine cells (arrows). (C) cryosection of colon showing an immunoreactive enteroendocrine cell with a neuropod (arrow). (D) Staining with IgG control revealed no immunoreactivity. (E) Submucosal ganglion in the ileum showing FMRFamide staining in nerve fibers. (F) Myenteric ganglion in the colon showing a FMRFamide-immunopositive nerve fiber. (G) Colchicine treatment diminished FMRFamide staining in the nerve fibers but did not reveal immunolabeling in the neuronal somata. (H) Staining of whole-mounts with IgG control revealed no immunoreactivity.

Fig. 3. Immunofluorescent double labeling of FMRFamide with the neural markers CGRP and tyrosine hydroxylase. (A-F) Absence of colocalization of FMRFamide with CGRP in the submucosal (A-C) and the myenteric (D-F) plexus. (G-L) Colocalization of FMRFamide with tyrosine hydroxylase in both the submucosal (G-I) and the myenteric plexus (J-L).

Fig. 4. RT-PCR was performed to reveal expression of receptors for proNPFF in BMMCs. mRNA of MrgprA1 and MrgprA4, but not of MrgprC11 or NPFF receptors, was detected in the BMMCs. Dorsal root ganglia served as positive control for Mrgprs and spinal cord for NPFF receptors (CTL: control).

Fig. 5. (A) Immunocytochemistry for the MrgA4 receptor on BMMCs. (B) Negative control.

Fig. 6. TEM images of unstimulated and stimulated BMMCs. (A) Unstimulated BMMC packed with typical electron-dense granules. (B) Partial degranulation of a BMMC following 30 min stimulation with NPAF (300 nM). (C) Further substantial loss of the granule content of BMMCs after stimulation with C48/80.

Fig. 7. NPAF-induced release of ß-hexosaminidase in BMMCs. The NPAF-induced release (A) is very subtle but statistically significant (one-way ANOVA, $p=0.043$, $n=5$ cultures), whereas the release induced by C48/80 (B) is clearly more prominent.

Fig. 8. NPAF-induced secretion of mMCP-1 from a BMMC measured by ELISA after 30 min of stimulation with different concentrations of NPAF.

Fig. 9. Live cell Ca^{2+} imaging. (A) BMMCs loaded with Fluo-4. (B) BMMCs showing spontaneous activity (arrows). (C) BMMCs stimulated with C48/80. (D) BMMCs after degranulation in response to C48/80.

Fig. 10. Representative live cell Ca^{2+}imaging recording (Fluo-4) of a BMMC showing normal spontaneous cell activity, increased Ca^{2+} oscillations after NPAF stimulation followed by a sudden increase in intracellular Ca^{2+} after C48/80.

Fig. 11. Increased Ca2+ activity after application of 300 nM NPAF. (A) Increase in Ca2+ peaks/min. (B) The ratio of peak frequency before and after NPAF treatment is not different in WT versus KO cultures. (C) The area under the curve is significantly increased after NPAF treatment but (D) the effect of NPAF application on the area under the curve did not differ between BMMCs derived from WT and cluster-KO mice.

Supplementary Fig 1

Morphological and immunocytochemical characterization of BMMC cultures

BMMC cultures were developed in order to investigate the expression of the ProNPFF precursor and its receptors in BMMCs and also to explore the response of MMCs to NPAF. BMMC cultures were maintained in TI3S medium for 14 days to promote cell survival, development and differentiation. Cell viability (assessed every two days using Nigrosin 2% staining) was invariably higher than 90%, although a small decrease was observed at days 2 and 4, followed by a steady increase plateauing at 97-98% viable cells (Fig. 1A). The cell culture consisted of low-adherent uniformly sized cells (Fig.

1B) with abundant presence of cytoplasmic granules (Figs. 1C,D). The presence of the MMC marker mMCP-1 in the cytoplasmic granules was confirmed using immunofluorescence (Fig. 1E), demonstrating that the bone marrow-derived cells had successfully developed into the morphological MMC phenotype during the culture period.

Supplementary Fig. 1. Morphological characterization of BMMCs. (A) Percentage of viable cells at different culture days. (B) Bright-field image of cultured cells showing BMMC morphology (day 12 of culture). (C, D) Leishman's staining showing the presence of acidic cytoplasmic granules at days 8 and 12 of culture. (E) Immunocytochemical detection of abundant amounts of mMCP-1 in the cytoplasmic granules of the BMMCs.

Table 1 List of antibodies used for immunocytochemistry and immunohistochemistry

Primary antibody			
Antigen	**Host**	**Dilution**	**Source**
Anti-FMRFamide	Rabbit	1:500	Merck-Millipore (AB15348)
Anti-calcitonin gene-related peptide (CGRP)	Goat	1:5000	Abcam (ab36001)
Anti-tyrosine hydroxylase	Sheep	1:500	Novus Biologicals, Littleton, CO, USA; NB300-110
Anti-mouse mast cell protease-1	Sheep	1:200	Moredun Scientific, Edinburgh, UK (MS-RM8)
Anti-Mas-related gene A4 (MrgprA4)	Rabbit	1:500	Avula et al., 2013

Secondary antibody		
Antigen	**Dilution**	**Source**
FITC-conjugated donkey anti-rabbit IgG	1:200	Jackson ImmunoResearch Laboratories
Cy3-conjugated donkey anti-goat IgG	1:500	Jackson ImmunoResearch Laboratories
Cy3-conjugated donkey anti-sheep IgG	1:500	Jackson ImmunoResearch Laboratories
FITC-conjugated donkey anti-sheep IgG	1:200	Jackson ImmunoResearch Laboratories
Cy3-conjugated donkey anti-rabbit IgG	1:500	Jackson ImmunoResearch Laboratories

.

Table 2. List of primers (FP= forward primer; RP= reverse primer) used for the RT-PCR experiments.

Gene	primer	Sequence 5'-3'	T^A (°C)	Amplicon size (bp)
ProNPFF	FP	CATGCACTTCTGCCAAACC	57	131
	RP	CAGTATGCCCACATTCCAGA		
mMrgprC11	FP	CTAGCATCCACAACCCCAG	58	236
	RP	TGTTTCCTGCCAGTCCAAC		
mMrgprA1	FP	GAGGAATGGGGGAAAGCAGC	57	289
	RP	TCTATGATGTGACCTAGGAGGAAG		
mMrgprA4	FP	ACCCTGATCCCAAACTTGATG	58	258
	RP	GCCTGTGATGTAGAGAACTGTC		
NPffr1	qMmuCID0016691		BioRad PrimePCR	
NPffr2	qMmuCID0010471		BioRad PrimePCR	

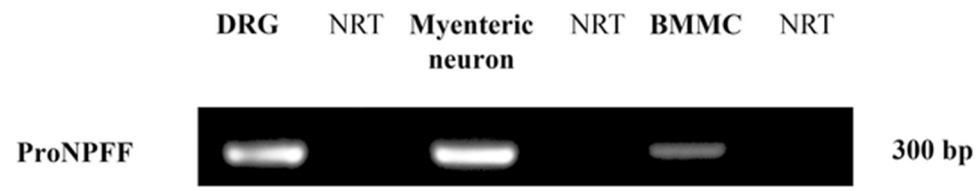

Fig. 1. mRNA for the NPAF precursor proNPFF is expressed in dorsal root ganglia, myenteric neurons and BMMCs (NRT: No Reverse Transcriptase reaction)

56x11mm (300 x 300 DPI)

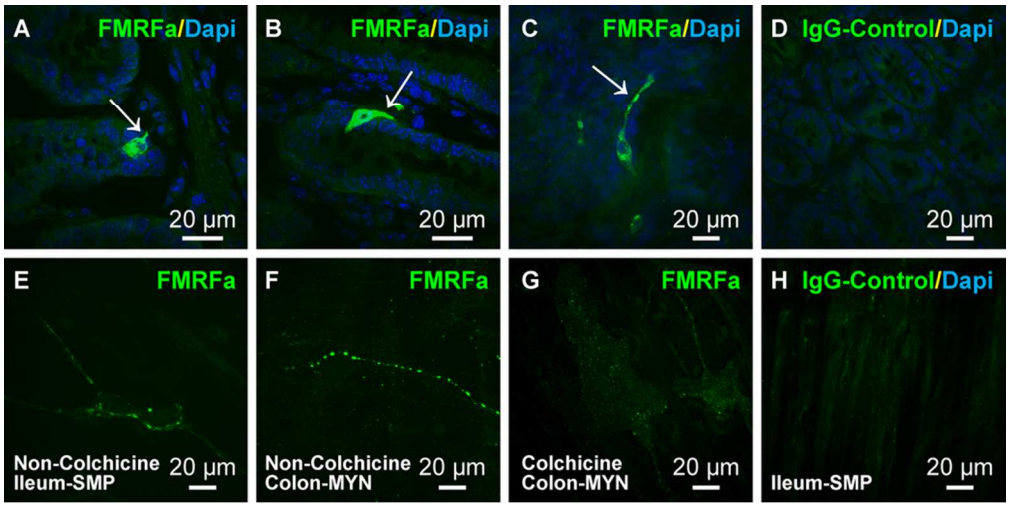

Fig. 2. Anti-FMRFamide-stained cryosections and whole-mounts. (A-B) Cryosections of colon (A) and ileum (B) showing expression of FMRFamides in enteroendocrine cells (arrows). (C) cryosection of colon showing an immunoreactive enteroendocrine cell with a neuropod (arrow). (D) Staining with IgG control revealed no immunoreactivity. (E) Submucosal ganglion in the ileum showing FMRFamide staining in nerve fibers. (F) Myenteric ganglion in the colon showing a FMRFamide-immunopositive nerve fiber. (G) Colchicine treatment diminished FMRFamide staining in the nerve fibers but did not reveal immunolabeling in the neuronal somata. (H) Staining of whole-mounts with IgG control revealed no immunoreactivity.

87x43mm (300 x 300 DPI)

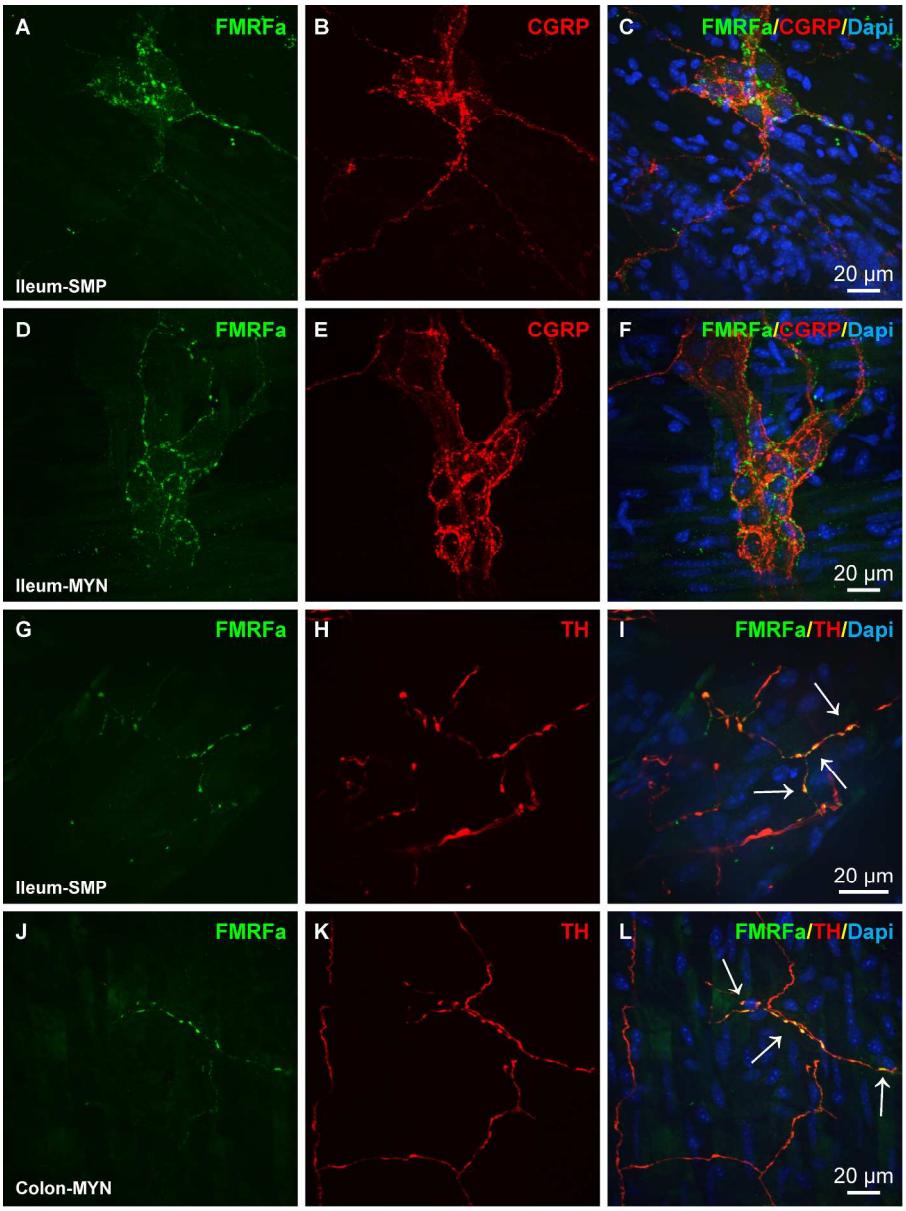

Fig. 3. Immunofluorescent double labeling of FMRFamide with the neural markers CGRP and tyrosine hydroxylase. (A-F) Absence of colocalization of FMRFamide with CGRP in the submucosal (A-C) and the myenteric (D-F) plexus. (G-L) Colocalization of FMRFamide with tyrosine hydroxylase in both the submucosal (G-I) and the myenteric plexus (J-L).

236x315mm (300 x 300 DPI)

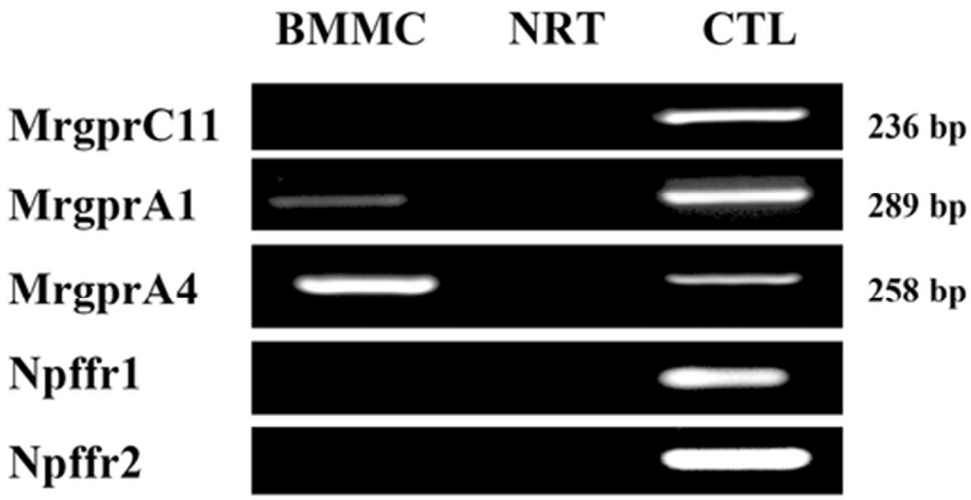

Fig. 4. RT-PCR was performed to reveal expression of receptors for proNPFF in BMMCs. mRNA of MrgprA1 and MrgprA4, but not of MrgprC11 or NPFF receptors, was detected in the BMMCs. Dorsal root ganglia served as positive control for Mrgprs and spinal cord for NPFF receptors (CTL: control).

44x23mm (300 x 300 DPI)

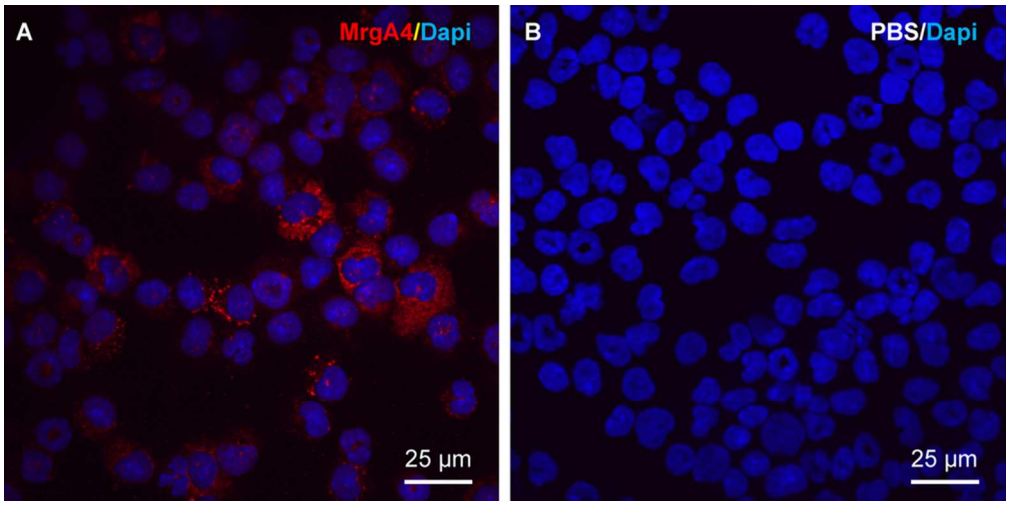

Fig. 5. (A) Immunocytochemistry for the MrgA4 receptor on BMMCs. (B) Negative control.

87x43mm (300 x 300 DPI)

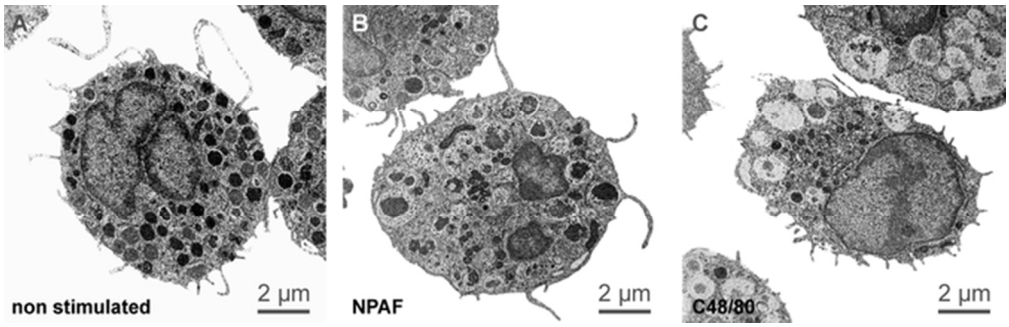

Fig. 6. TEM images of unstimulated and stimulated BMMCs. (A) Unstimulated BMMC packed with typical electron-dense granules. (B) Partial degranulation of a BMMC following 30 min stimulation with NPAF (300 nM). (C) Further substantial loss of the granule content of BMMCs after stimulation with C48/80.

56x18mm (300 x 300 DPI)

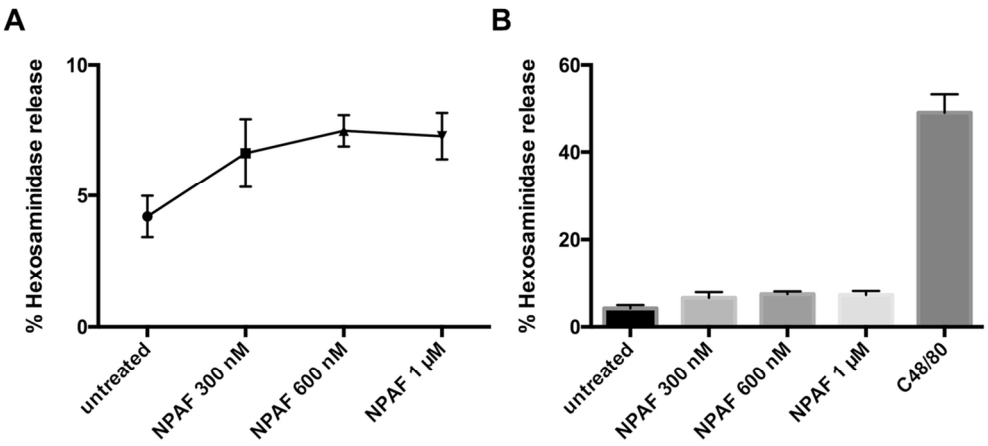

Fig. 7. NPAF-induced release of ß-hexosaminidase in BMMCs. The NPAF-induced release (A) is very subtle but statistically significant (one-way ANOVA, p=0.043, n=5 cultures), whereas the release induced by C48/80 (B) is clearly more prominent.

55x25mm (600 x 600 DPI)

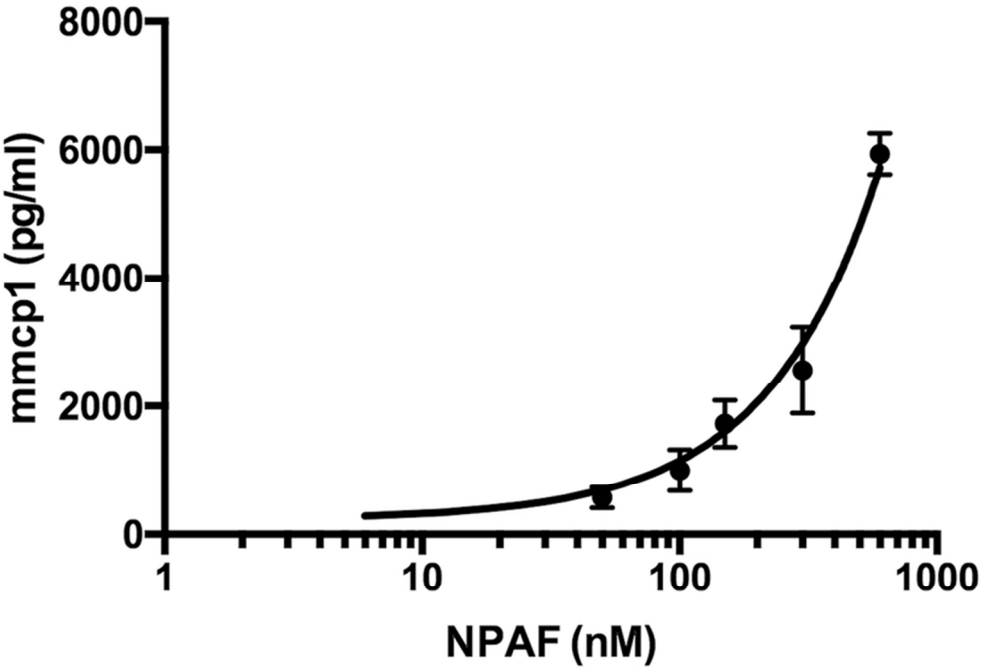

Fig. 8. NPAF-induced secretion of mMCP-1 from a BMMC measured by ELISA after 30 min of stimulation with different concentrations of NPAF.

35x24mm (600 x 600 DPI)

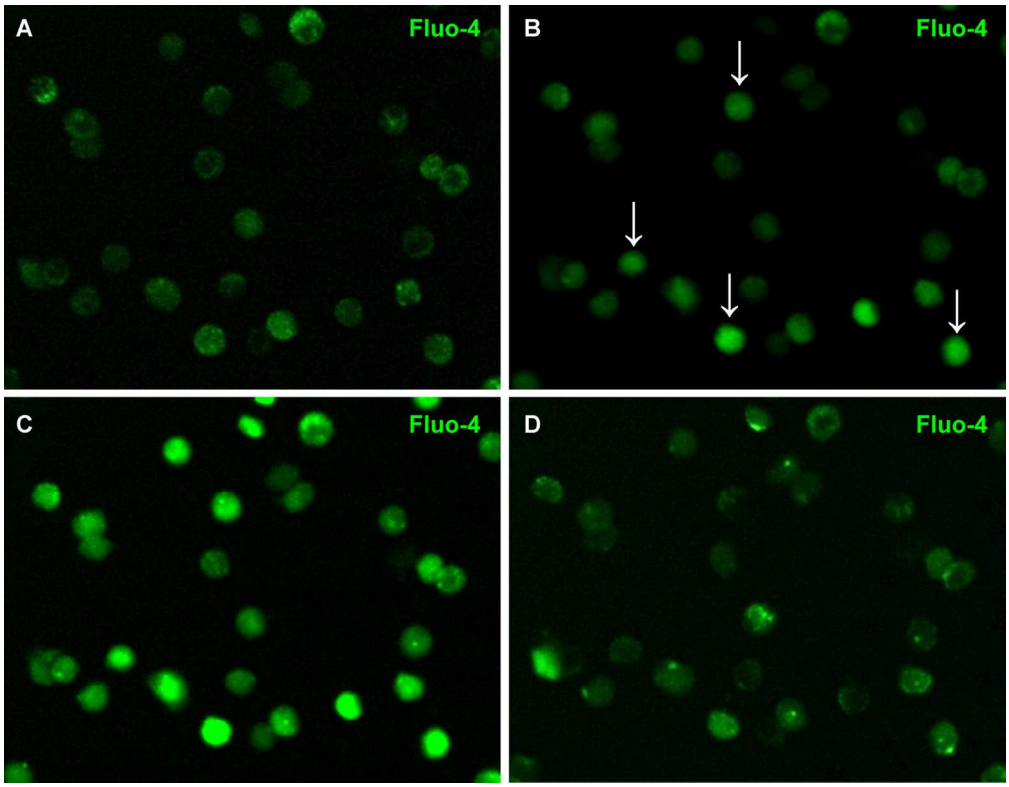

Fig. 9. Live cell Ca2+ imaging. (A) BMMCs loaded with Fluo-4. (B) BMMCs showing spontaneous activity (arrows). (C) BMMCs stimulated with C48/80. (D) BMMCs after degranulation in response to C48/80.

137x106mm (300 x 300 DPI)

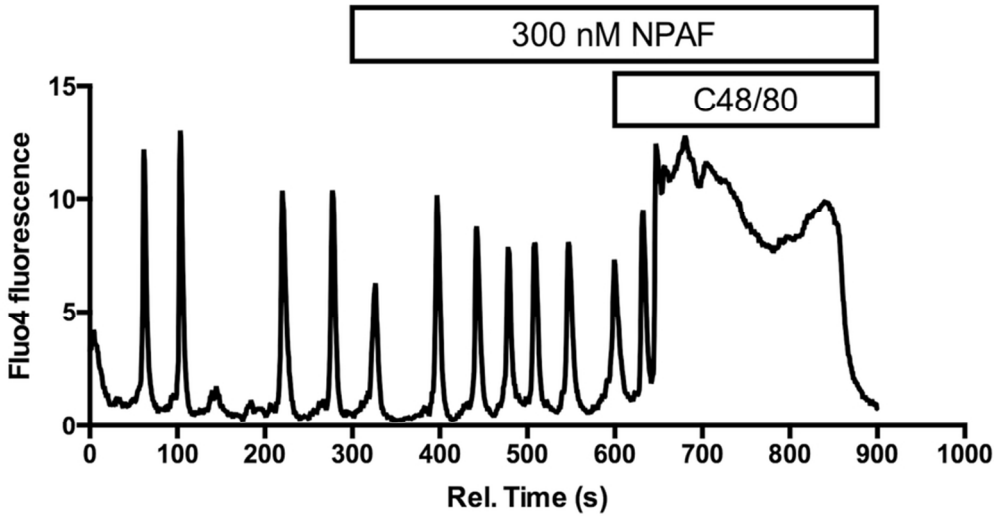

Fig. 10. Representative live cell Ca2+imaging recording (Fluo-4) of a BMMC showing normal spontaneous cell activity, increased Ca2+ oscillations after NPAF stimulation followed by a sudden increase in intracellular Ca2+ after C48/80.

39x20mm (600 x 600 DPI)

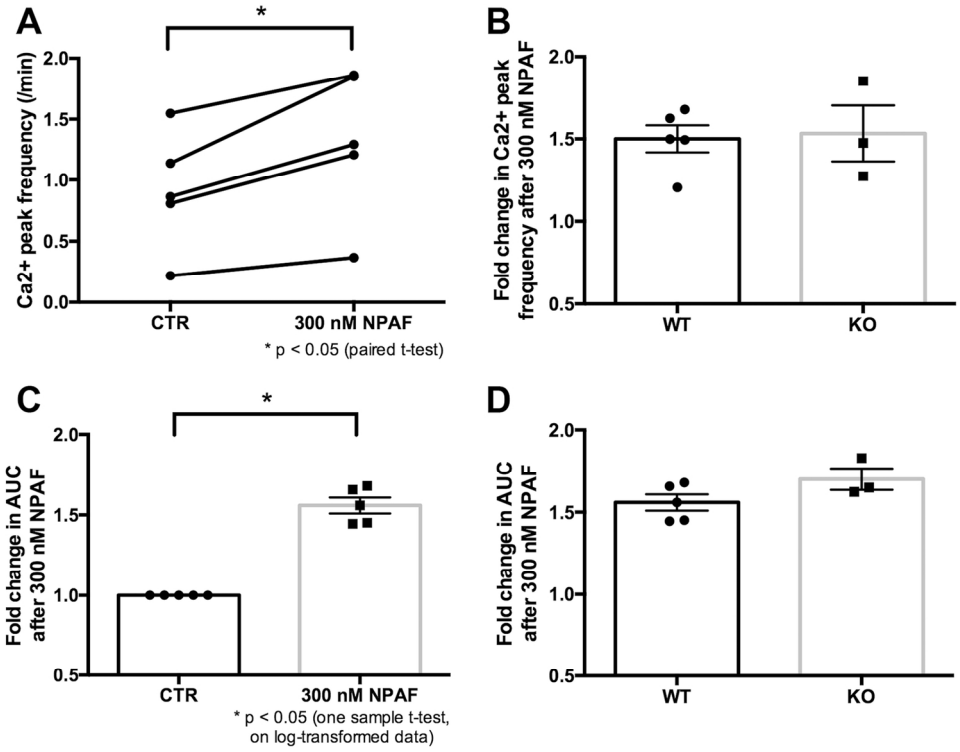

Fig. 11. Increased Ca2+ activity after application of 300 nM NPAF. (A) Increase in Ca2+ peaks/min. (B) The ratio of peak frequency before and after NPAF treatment is not different in WT versus KO cultures. (C) The area under the curve is significantly increased after NPAF treatment but (D) the effect of NPAF application on the area under the curve did not differ between BMMCs derived from WT and cluster-KO mice.

69x54mm (600 x 600 DPI)